Int J Clin Exp Med 2016;9(8):16052-16060
www.ijcem.com /ISSN:1940-5901/IJCEM0028650

Original Article

Contrast-enhanced ultrasound features in papillary thyroid carcinomas with different sizes

Yi Liu[1*], Hua Liu[2*], Shufei Jiang[1], Changlin Qian[2], Zhihua Han[3], Fenghua Li[1], Jianguo Xia[1]

Departments of [1]Ultrasound, [2]General Surgery, South Campus, Renji Hospital, School of Medicine, Shanghai Jiao Tong University, 2000 Jiangyue Road, Shanghai 201112, China; [3]Department of Cardiology, Ninth People's Hospital, School of Medicine, Shanghai Jiao Tong University, 639 Zhizaoju Road, Shanghai 200011, China. [*]Equal contributors.

Received March 18, 2016; Accepted June 12, 2016; Epub August 15, 2016; Published August 30, 2016

Abstract: Objective: This study aims to analyze the differences in the contrast-enhanced ultrasound features between papillary thyroid microcarcinoma (PTMC) and papillary thyroid carcinoma (PTC) (diameter > 10 mm). Methods: A total of 59 thyroid cancer patients with 63 pathologically confirmed thyroid cancer nodules were enrolled in this retrospective study. Contrast-enhanced ultrasound features were evaluated for each nodule. Results: Patients with PTMC more frequently exhibited dotted enhancement, well-defined margins, and hypoenhancement, while patients with PTC (diameter > 10 mm) more often exhibited diffuse heteroenhancement, ill-defined margins, isoenhancement and hypoenhancement (*P*=0.001, 0.000, and 0.000, respectively). Peak intensity, wash in slope, and area under the curve were significantly higher in PTC (diameter > 10 mm) than in PTMC (*P*=0.000, 0.000, and 0.005, respectively); rising time, time to peak, and time from peak to one half were significantly shorter in PTC (diameter > 10 mm) than in PTMC (*P*=0.030, 0.003, and 0.002, respectively). Multivariate stepwise logistic regression analysis revealed that peak intensity, time from peak to one half and wash in slope were the most significantly different parameters (odds ratio =6.392, *P*=0.001; odds ratio =0.777, *P*=0.011 and odds ratio =0.021, *P*=0.049, respectively). Conclusion: The distinct differences of contrast-enhanced ultrasound in PTMC and PTC (diameter > 10 mm) provide important insights into the pathology of them, which is essential for optimal clinical diagnosis and treatment.

Keywords: Contrast-enhanced ultrasound, qualitative pattern, quantitative parameter, papillary thyroid microcarcinoma, papillary thyroid carcinoma, pathology

Introduction

Thyroid nodules occur frequently in the general population. The incidence of thyroid cancer has increased steeply in recent years; consequently, the detection of malignant thyroid nodules during an ultrasonographic examination is important. Gray-scale ultrasonography (GSUS) and color Doppler ultrasonography (CDUS) are conventional imaging techniques used for the detection of malignant thyroid nodules [1-4]. However, the accuracy of these two modalities is not high, and they have limited effectiveness in detecting malignant thyroid nodules [5].

Recently, the introduction of CEUS as a promising tool for the study of the microvascular flow pattern in thyroid lesions has provided valuable indicators regarding the differentiation of benign from malignant thyroid nodules [6-8]. For example, Zhang et al. [6] concluded that the enhancement patterns of CEUS were helpful in the differential diagnosis of thyroid nodules. Ring enhancement was valuable in the diagnosis of benign thyroid nodules, whereas heterogeneous enhancement was useful in the detection of malignant thyroid nodules. Nemec et al. [7] reported that there was a significant difference (*P*<0.001) in CEUS enhancement data between benign and malignant thyroid nodules. Quantitative analysis using CEUS contributed in the differentiation of benign from malignant thyroid nodules. These previous studies elucidated the diagnostic value of CEUS; however, little is known about the relationship of CEUS features between PTMC and PTC (diameter [d] > 10 mm). If the maximum d of a PTC tumor is ≤10 mm, it is defined by the World Health

Table 1. Univariate analysis of patients characteristics of PTMC and PTC (d > 10 mm)

Characteristics	PTMC	PTC (d > 10 mm)	*P* value
Gender			
Male	7	2	0.301
Female	30	20	
Age (yrs)	50±11	48±13	0.260
Tumor size (mm)	7.19±1.30	17.46±7.47	0.000

Organization (WHO) as a PTMC. Recent studies have shown that tumor size was one of the significant prognostic factors for thyroid cancer, and it should be taken into account in its management. A larger lesion size (d > 10 mm) has been reported to be the best predictor of extrathyroidal extension and cervical lymph node metastasis (CLNM) [9-11]. For example, Kim et al. evaluated 354 PTC patients. They found that tumor diameters > 10 mm and hypoechogenicity predicted the presence of central compartment lymph node metastases [11]. We hypothesize that there is a linkage of CEUS features between PTMC and PTC tumors (d > 10 mm). Consequently, the aim of this study was to analyze the differences in CEUS qualitative patterns and quantitative features between PTMC and PTC tumors (d > 10 mm) to evaluate the potential of CEUS in their characterization.

Materials and methods

Study population

From July 2014 to October 2015, 59 patients (9 men and 50 women) aged 26-69 years (mean, 49 years) with 63 thyroid nodules were verified as having PTC by surgical pathology. All patients were selected preoperatively on the basis of suspicion of malignant thyroid lesions on conventional ultrasonography (US). Thirty-eight patients underwent US-guided fine-needle aspiration cytology (FNAC) preoperatively. Twenty-one patients did not underwent FNAC preoperatively. They underwent surgery due to suspicious malignant nodules on US findings. All patients underwent preoperative CEUS examination and were evaluated retrospectively in this study. The study was approved by the Ethics Committee of Shanghai Renji Hospital, School of Medicine, Shanghai Jiao Tong University, and written informed consent was obtained from all patients before undergoing CEUS. Of these patients, 55 had solitary malignant lesions, 3 had two malignant lesions, and 1 had three malignant lesions, while the d of one malignant nodule was <5 mm and was excluded. The inclusion criteria were as follows: nodules > 5 mm (for nodules <5 mm, it was difficult to maintain the imaging plane unchanged during CEUS because of breathing and arterial pulsations); and age > 18 years. The exclusion criteria were as follows: previous side effects caused by contrast agents; pregnancy; breastfeeding; and severe cardiopulmonary insufficiency. According to tumor size, the enrolled patients were divided into two groups, namely the PTMC and PTC groups.

Ultrasonographic examination

A Philips iU22 ultrasonography system (Philips, Bothell, WA, USA) equipped with a L12-5 transducer was used for conventional ultrasound examination and a L9-3 transducer were used for CEUS. Before CEUS, the thyroid nodule and the lymph nodes were scanned carefully using GSUS and CDUS. The depth, gain, and focal zone were optimized during examination. The nodule's maximum diameter was measured. Then, the suspect malignant nodule was examined using CEUS. The largest section of the nodule was selected for evaluation. The contrast agent used was Sulphurhexafluoride (SonoVue, Bracco, Milan, Italy). A contrast agent in a 2.4-mL suspension was injected as a bolus within 1 to 2 seconds through the antecubital vein followed by a 5-mL 0.9% saline solution flush. CEUS was used in low mechanical index mode (0.07); the focus was always set at the bottom of the nodule plane. When CEUS was initiated, the imaging section was maintained unchanged for each patient. The contrast-enhanced images of each suspect malignant nodule were observed continuously for 3 min. Digital video clips were stored on the hard disk of the machine in DICOM format. All CEUS images were analyzed separately by two experienced sonographers. All of the image reviewers were blinded to the patient clinical information and pathological findings.

Qualitative CEUS pattern analysis

CEUS enhancement patterns were as follows. (1) The degree of contrast agent distribution was classified into diffuse enhancement and dotted enhancement. Diffuse enhancement

Table 2. Comparison of qualitative CEUS pattern features between PTMC and PTC (d > 10 mm)

Patterns	PTMC (n, %)	PTC (d > 10 mm) (n, %)	*P* value
The degree of contrast agent distribution			
Diffuse heterogeneous enhancement	14 (35.0)	18 (78.3)	
Diffuse homogeneous enhancement	3 (7.5)	3 (13.0)	0.001
Dotted enhancement	23 (57.5)	2 (8.7)	
Margin type			
Well-defined margin	22 (55.0)	2 (8.7)	0.000
Ill-defined margin	18 (45.0)	21 (91.3)	
Enhancement degree			
Hypoenhancement	37 (92.5)	11 (47.8)	
Isoenhancement	3 (7.5)	10 (43.5)	0.000
Hyperenhancement	0 (0)	2 (8.7)	

was defined as wide distribution of the contrast agent throughout the entire nodule with heterogeneous or homogeneous enhancement. Diffuse heterogeneous enhancement was defined as diffuse and heterogeneous enhancement of the nodule at the peak time of enhancement. Diffuse homogeneous enhancement was defined as diffuse and homogeneous enhancement of the nodule at the peak time of enhancement. Dotted enhancement was defined as enhancement involving tiny and separate spots of contrast agent distributed throughout the nodule. (2) The margin type was divided into a well-defined margin and an ill-defined margin. (3) The degree of enhancement was classified as isoenhancement, hypoenhancementor hyperenhancement. It was defined as isoenhancement when the nodule echogenicity was equal to that of the thyroid parenchyma. It was defined as hypoenhancement when the nodule echogenicity was lower than that of the thyroid parenchyma. It was defined as hyperenhancement when the nodule echogenicity was higher than that of the thyroid parenchyma.

Quantitative CEUS parameter analysis

The time-intensity curve (TIC) quantitative analysis was carried out using Q-LAB software (Philips Medical Systems, Bothell, WA). A region of interest was drawn within the whole area of the nodule. The signal intensity of each nodule was expressed in decibels (dB). The TIC indices were as follows: peak intensity (PI [in dB]) defined as the curve's maximum intensity minus the baseline intensity (BI); rising time (RT [in sec]) defined as the time from 5% of the curve's maximum intensity to 95% of that; time to peak (TTP [in sec]) defined as the time the lesions reach the curve's maximum intensity; wash in slope (WIS [in dB/sec]) is calculated by subtracting the intensity at 5% of the curve's maximum intensity from that at 95% of the curve's maximum intensity, and dividing this by the RT; time from peak to one half (TPH [in sec]) defined as the time from the highest intensity of the curve to when that drops to 50%; and area under the time-intensity curve (AUC [in dBsec]).

Statistical analysis

Statistical analysis was performed using SPSS version 17.0 software (SPSS Inc., Chicago, IL, USA). Qualitative data were compared using the Chi-square or Fisher P tests. Quantitative data were expressed as the mean (± standard deviation [SD]) and analyzed using the Student's t test. All data that were confirmed to be statistically significant on univariate analysis were further analyzed using multivariate logistic regression. A p value <0.05 was considered as being statistically significant.

Results

Demographic characteristics

Patient characteristics are detailed in **Table 1**. Univariate analysis demonstrated a significant difference in tumor size between the PTMC and PTC groups (7.19±1.30 mm vs 17.46±7.47 mm; P=0.000), while there was no significant difference in patient age and sex between the two groups (P=0.260 and 0.301, respectively).

Qualitative CEUS pattern analysis in PTMC and PTC tumors

As shown in **Table 2**, patients with PTMC tumors more often exhibited dotted enhancement, a well-defined margin, and hypoenhancement, while patients with PTC tumors more often exhibited diffuse heteroenhancement, an ill-

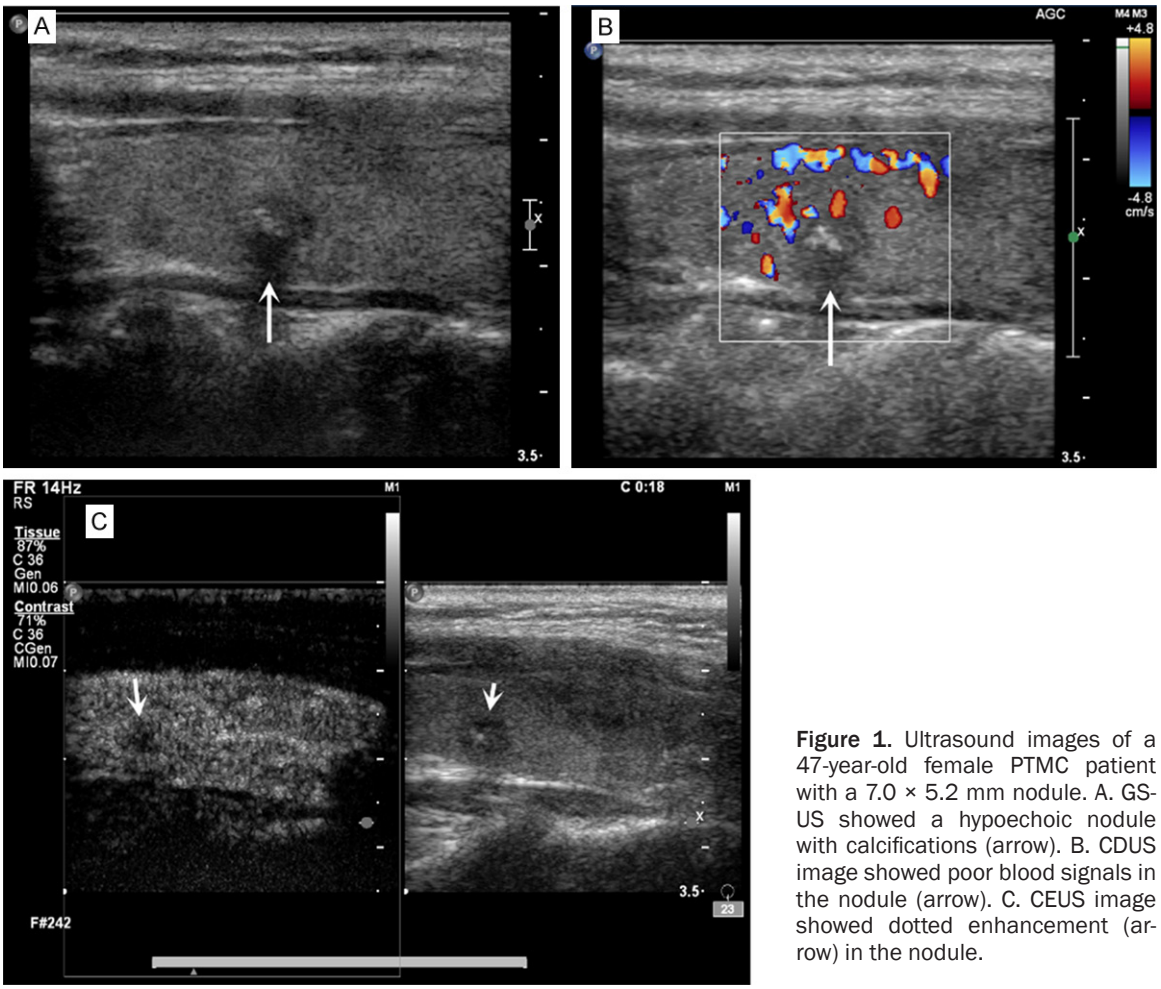

Figure 1. Ultrasound images of a 47-year-old female PTMC patient with a 7.0 × 5.2 mm nodule. A. GS-US showed a hypoechoic nodule with calcifications (arrow). B. CDUS image showed poor blood signals in the nodule (arrow). C. CEUS image showed dotted enhancement (arrow) in the nodule.

defined margin, isoenhancement and hypoenhancement (*P*=0.001, 0.000, and 0.000, respectively). A total of 23 (57.5%) patients with PTMC tumors exhibited dotted enhancement, 22 (55.0%) with PTMC tumors exhibited a well-defined margin, and 37 (92.5%) with PTMC tumors exhibited hypoenhancement. A total of 18 (78.3%) patients with PTC tumors showed diffuse heteroenhancement, 21 (91.3%) with PTC tumors showed an ill-defined margin, 10 (43.5%) with PTC tumors showed isoenhancement, and 11 (47.8%) with PTC tumors showed hypoenhancement (**Figures 1** and **2**).

Quantitative CEUS parameter analysis of PTMC and PTC tumors

The values of the quantitative CEUS parameters are detailed in **Table 3**. Patients with PTMC and PTC tumors showed significant differences in all of the quantitative CEUS parameters. The PI, WIS, and AUC were significantly higher in PTC tumors than in PTMC tumors (*P*=0.000, 0.000, and 0.005, respectively), whereas the RT, TTP, and TPH were significantly shorter in PTC tumors than in PTMC tumors (*P*=0.030, 0.003, and 0.002, respectively).

Multivariate logistic regression analysis

Multivariate logistic regression analysis revealed that WIS was the most significantly different parameter between the PTMC and PTC groups (odds ratio [OR] =0.008; 95% confidence interval [CI], 0.000-0.532; *P*=0.024; **Table 4**). Subsequently, we analyzed the above data using multivariate stepwise logistic regression. It was found that PI (OR=6.392; 95% CI, 2.111-19.355; *P*=0.001), TPH (OR=0.777; 95% CI, 0.641-0.943; *P*=0.011), and WIS (OR=0.021; 95% CI, 0.000-0.979; *P*=0.049) differed significantly between the PTMC and PTC groups. Among these parameters, PI was the most significantly different (**Table 5**).

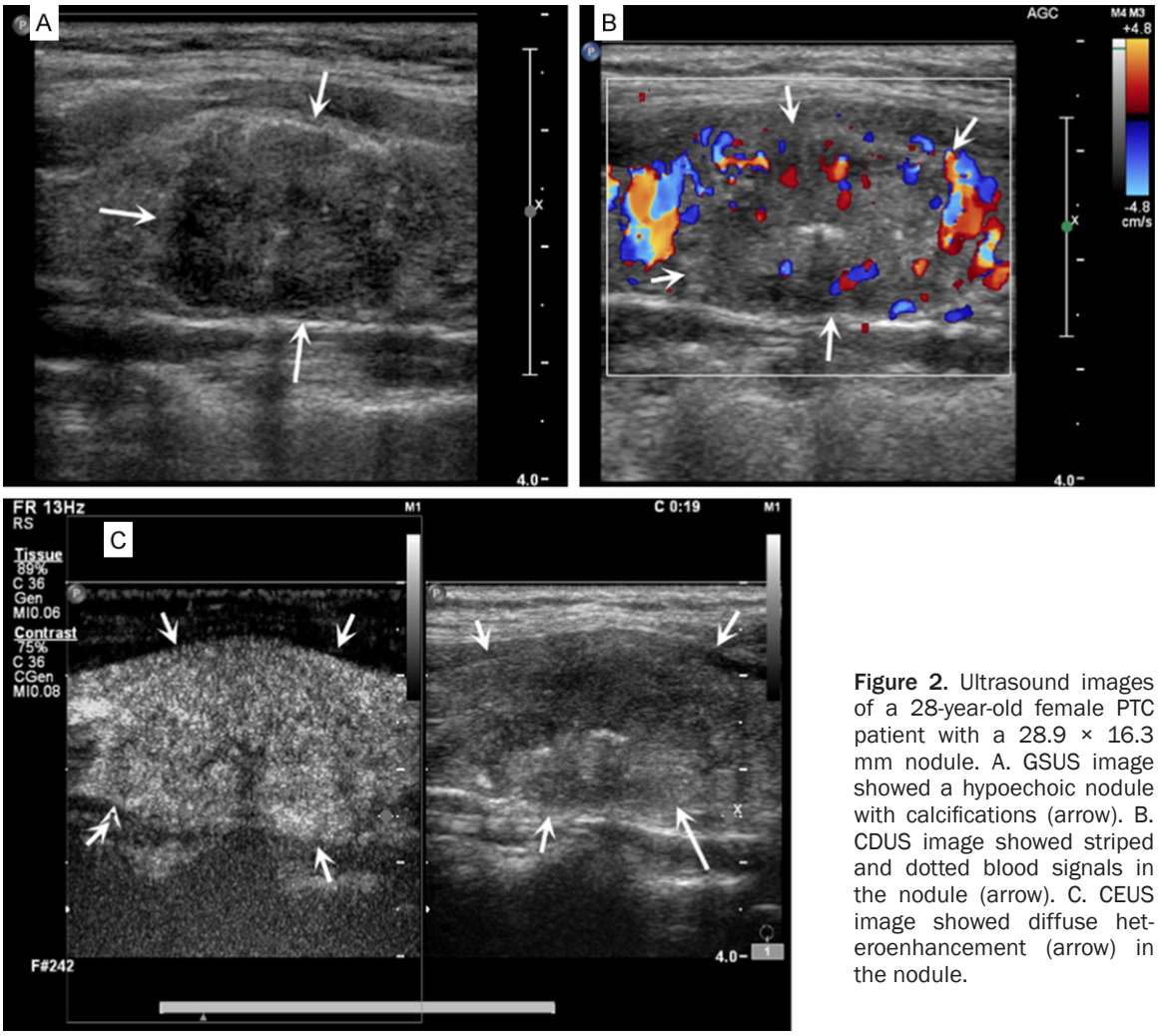

Figure 2. Ultrasound images of a 28-year-old female PTC patient with a 28.9 × 16.3 mm nodule. A. GSUS image showed a hypoechoic nodule with calcifications (arrow). B. CDUS image showed striped and dotted blood signals in the nodule (arrow). C. CEUS image showed diffuse heteroenhancement (arrow) in the nodule.

Table 3. Comparison of quantitative CEUS parameter features between PTMC and PTC (d > 10 mm)

Parameters	PTMC (Mean ± SD)	PTC (d > 10 mm) (Mean ± SD)	*P* value
RT (sec)	11.01±10.77	6.99±2.80	0.030
TTP (sec)	71.36±25.79	54.74±14.07	0.003
PI (dB)	6.93±1.88	9.84±1.93	0.000
WIS (dB/sec)	0.84±0.53	1.41±0.57	0.000
TPH (sec)	29.50±13.51	21.88±5.47	0.002
AUC (dBsec)	575.52±188.50	727.94±221.06	0.005

RT: rising time; TTP: time to peak; PI: peak intensity; WIS: wash in slope; TPH: time from peak to one half; AUC: area under the curve.

The TIC features of PTMC and PTC tumors

The shape of all of the TICs indicated a rapid and high level of enhancement of the wash-in curve together with a quick wash out; this was the characteristic feature of PTC tumors. A mild and low level of enhancement of the wash-in curve combined with a delayed wash out was the characteristic TIC feature of PTMC tumors (**Figure 3**).

Discussion

The present study demonstrated that the qualitative CEUS patterns and quantitative features were distinctly different in the PTMC and PTC tumors, especially regarding the three quantitative parameters: PI, TPH, and WIS. Among these three parameters, PI played a key role in characterizing the PTMC and PTC tumors. These findings were similar to data previously published in some aspects. Previous studies have shown that a larger thyroid tumor size was one of the statistically significant prognostic factors for thyroid cancer. Wang et al. evaluated the ultrasonographic features of 513 PTC nodules

Table 4. Multivariate logistic analysis of the CEUS qualitative patterns and quantitative parameters

Patterns and parameters	OR	95% CI	*P* value
The degree of contrast agent distribution	1.118	0.256-4.872	0.882
Margin type	4.033	0.093-174.042	0.468
Enhancement degree	14.078	0.900-220.149	0.059
RT	1.322	0.821-2.129	0.250
TTP	0.787	0.570-1.087	0.146
PI	12.220	0.972-153.684	0.053
WIS	0.008	0.000-0.532	0.024
TPH	0.816	0.640-1.039	0.098
AUC	0.988	0.958-1.019	0.446

RT: rising time; TTP: time to peak; PI: peak intensity; WIS: wash in slope; TPH: time from peak to one half; AUC: area under the curve; OR: odds ratio; CI: confidence interval.

Table 5. Multivariate stepwise logistic analysis of the CEUS qualitative patterns and quantitative parameters

Parameters	OR	95% CI	*P* value
PI	6.392	2.111-19.355	0.001
TPH	0.777	0.641-0.943	0.011
WIS	0.021	0.000-0.979	0.049

PI: peak intensity; TPH: time from peak to one half; WIS: wash in slope; OR: odds ratio; CI: confidence interval.

[12]. They found that larger tumor size (d > 10 mm) was one of the significant factors for predicting CLNM ($P<0.05$; OR=2.093) [12]. Lee et al. studied 320 PTC patients with suspected extrathyroidal extension, and found that a larger tumor size ($P<0.001$) was one of the best predictors of extrathyroidal extension [10]. CEUS, a non-invasively diagnostic imaging technique, has already been recommended for clinical use. It can contribute effectively in the evaluation of tumor microvascularity [13, 14]. However, few studies have compared CEUS features between PTMC and PTC tumors. Hence, we used both qualitative and quantitative analyses with CEUS to explore the characteristics of these tumors.

The qualitative CEUS results indicated that, in the PTMC group, CEUS mainly showed dotted enhancement, well-defined margins, and hypoenhancement; in the PTC group, CEUS mainly exhibited diffuse heteroenhancement, ill-defined margins, isoenhancement and hypoenhancement. The CEUS features can provide valuable information on the blood supply inside nodules. The degree of perfusion of the contrast agent is determined by the amount of new blood vessels. Previous studies have shown that growth of the tumor takes place in two stages, namely the pre-vascular stage and the vascular stage [15, 16]. The pre-vascular stage encompasses the tumor's slow-growing phase in the absence of blood vessels. The vascular stage encompasses the tumor's fast-growing phase in the presence of blood vessels. With fewer blood vessels than PTC tumors, PTMC tumors exhibited the most hypoenhancement and dotted enhancement under CEUS because of the presence of intranodular necrosis and fibrosis. Massive new blood vessels develop to meet the requirements of tumor growth. Thus, isoenhancement and hyperenhancement were observed more in PTC tumors than in PTMC tumors. In addition, PTC tumors are also associated with intranodular necrosis and fibrosis, but the ratio of blood vessels in PTC tumors is more than that in PTMC tumors; thus, they always exhibit the characteristics of diffuse heterogeneous enhancement. Generally, in thyroid cancer, new vessels distribute in the surrounding and central areas. Along with thyroid tumor growth, the distribution of massive blood vessels is centered in the tumor's surrounding area, and the tumor always grows invasively outwards; this contributes to the formation of the tumor's ill-defined margin in CEUS involving PTC. In contrast, in the PTMC group, because of the presence of fewer blood vessels in the tumor including the surrounding area, most tumors showed well-defined margins when visualized using CEUS [17]. These findings were in agreement with those of similar studies to some degree. Bartolotta et al. [19] revealed that the CEUS enhancement pattern of thyroid cancer was closely related to nodule size; enhancement appeared to be mostly absent enhancement in nodules with a d<10 mm, dotted enhancement was evident in nodules with a d of 10-20 mm diameter, and diffuse enhancement was present in nodules with a d > 20 mm [18]. The reason for these findings may be that

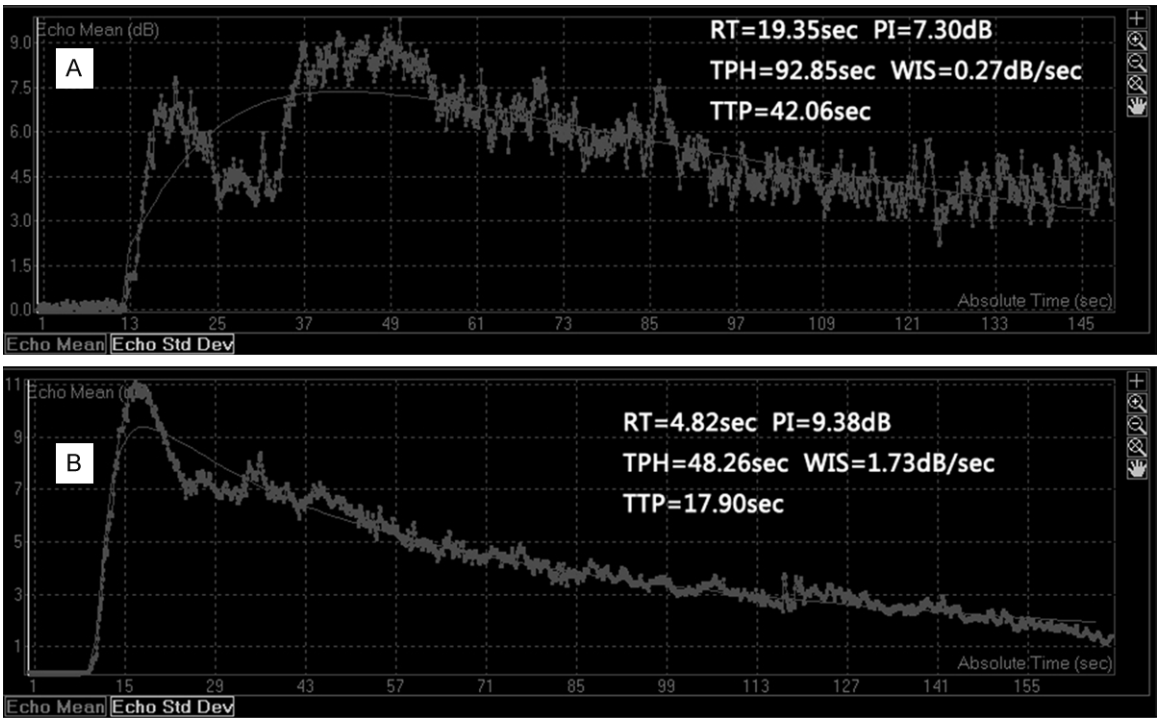

Figure 3. The different TIC features in CEUS of PTMC and PTC (d > 10 mm). A. TIC of PTMC, showing slower wash-in, prolonged wash-out and lower PI. B. TIC of PTC (d > 10 mm), showing rapider wash-in, accelerated wash-out and higher PI.

in smaller thyroid cancer nodules, the growth rate of neoangiogenetic vessels is slower than the rate of cancer cell proliferation. However, in our study, we confirmed that the CEUS enhancement pattern of PTMC was mainly dotted enhancement, whereas mainly diffuse heteroenhancement was observed in PTC tumors with a d > 20 mm, and PTC tumors with a d of 10-20 mm. More importantly, the quantitative CEUS features for PTMC and PTC tumors have not been previously explored; so we highlighted the distinction in quantitative CEUS features between the PTMC and PTC groups.

In the present study, PTC tumors showed a shorter RT, TTP, and TPH, a steeper WIS, and a higher PI than PTMC tumors. The shorter the RT and TTP, the more rapid the filling-in rate of the contrast agent. The steeper the WIS, the more rapid the wash-in rate of contrast agent. The shorter the TPH, the more rapid the wash-out rate of the contrast agent. Previous studies have shown that RT and TTP can accurately reflect the blood supply component of liver tumors [19, 20]; the blood supply ratio of the hepatic artery and portal vein can determine this. When the proportion of the hepatic artery blood supply is larger, the RT is faster and the TTP is shorter. Conversely, when the proportion of the portal vein blood supply is increasing, the RT is slower and the TTP is prolonged. Consequently, we hypothesized that along with thyroid cancer growth, the artery blood supply may be increased significantly as compared with the venous blood supply. Thus, RT and TTP were shorter in patients with PTC than in patients with PTMC. Additionally, because of the presence of massive neocapillaries, a large amount of contrast agent would concentrate in the tumor, leading to the significantly high PI and steep WIS in PTC tumors. We found that PTC tumors showed more rapid washout than PTMC tumors. The reasons for this remain unclear. Some studies involving the liver have reported the possible causes. Yang et al. [21] pointed out that early hepatocellular carcinoma was usually fed by portal veins, and as a result the wash-out time was prolonged. The metastases from hepatocellular carcinoma generally exhibited rapid wash-out. This may be related to the increased tumor arterial vascular supply. Kong et al. [22] demonstrated that smaller intrahepatic cholangiocarcinoma nodules had a larger number of tumor vessels, and that homoge-

neous arterial enhancement and rapid washout were observed. Hence, we postulated that that there was a greater increase in tumor arterial vessels in PTC than in PTMC, which led to faster washout in PTC.

Multivariate regression analysis revealed that PI, TPH, and WIS differed significantly between the PTMC and PTC groups. Among these, PI was found to be the most significantly different parameter regarding the characterization of PTMC and PTC. This phenomenon is not fully understood. We postulated that PI may be the best parameter that can reflect tumor artery supply. Because of the presence of massive new capillaries, especially arteries, a large amount of contrast agent would concentrate in the tumor; then tumor perfusion would be increased, leading to the significantly high PI in PTC tumors [23].

The limitations of our study were as follows. First, the sample size was relatively small. A multicenter study involving a large sample size should be considered in the future to strengthen the findings. Second, in our study there was a lack of similar data for PTMC and PTC from conventional US and histological confirmation about perfusion changes in CEUS; this will be required in a future study. Third, because thyroid cancer of other pathological types was not encountered in the current study, a large series study including thyroid cancer of all pathological types is needed.

Conclusion

PTMC and PTC may display various enhancement patterns and different enhancement parameters on CEUS, especially regarding the three quantitative parameters: PI, TPH, and WIS. These changes may be as a result of similar pathological changes. CEUS may have the potential to provide essential information on the characteristics of PTMC and PTC and indirect information on the pathological mechanisms involved, which is essential for optimal clinical diagnosis and treatment.

Acknowledgements

This work was made possible by Scientific Research Initial Foundation of Renji Hospital South Campus grant 2014QDM03.

Disclosure of conflict of interest

None.

Address correspondence to: Jianguo Xia, Departments of Ultrasound, South Campus, Renji Hospital, School of Medicine, Shanghai Jiao Tong University, 2000 Jiangyue Road, Shanghai 201112, China. E-mail: pleasure1019@sina.com

References

[1] Gharib H, Papini E, Paschke R, Duick DS, Valcavi R, Hegedus L and Vitti P. American Association of Clinical Endocrinologists, Associazione Medici Endocrinologi, and European Thyroid Association Medical guidelines for clinical practice for the diagnosis and management of thyroid nodules: executive summary of recommendations. Endocr Pract 2010; 16: 468-475.

[2] Frates MC, Benson CB, Charboneau JW, Cibas ES, Clark OH, Coleman BG, Cronan JJ, Doubilet PM, Evans DB, Goellner JR, Hay ID, Hertzberg BS, Intenzo CM, Jeffrey RB, Langer JE, Larsen PR, Mandel SJ, Middleton WD, Reading CC, Sherman SI and Tessler FN. Management of thyroid nodules detected at US: Society of Radiologists in Ultrasound consensus conference statement. Radiology 2005; 237: 794-800.

[3] Moon WJ, Jung SL, Lee JH, Na DG, Baek JH, Lee YH, Kim J, Kim HS, Byun JS and LeeDH. Benign and malignant thyroid nodules: US differentiation--multicenter retrospective study. Radiology 2008; 247: 762-770.

[4] Hoang JK, Lee WK, Lee M, Johnson D and Farrell S. US Features of thyroid malignancy: pearls and pitfalls. Radiographics 2007; 27: 847-860.

[5] Peccin S, de Castsro JA, Furlanetto TW, Furtado AP, Brasil BA and Czepielewski MA. Ultrasonography: is it useful in the diagnosis of cancer in thyroid nodules? J Endocrinol Invest 2002; 25: 39-43.

[6] Zhang B, Jiang YX, Liu JB, Yang M, Dai Q, Zhu QL and Gao P. Utility of contrast-enhanced ultrasound for evaluation of thyroid nodules. Thyroid 2010; 20: 51-57.

[7] Nemec U, Nemec SF, Novotny C, Weber M, Czerny C and Krestan CR. Quantitative evaluation of contrast-enhanced ultrasound after intravenous administration of a microbubble contrast agent for differentiation of benign and malignant thyroid nodules: assessment of diagnostic accuracy. Eur Radiol 2012; 22: 1357-1365.

[8] Ma JJ, Ding H, Xu BH, Xu C, Song LJ, Huang BJ and Wang WP. Diagnostic performances of various gray-scale, color Doppler, and contrast-

enhanced ultrasonography findings in predicting malignant thyroid nodules. Thyroid 2014; 24: 355-363.
[9] Erol V, Makay O, Icoz G, Kose T, Yararbas U, Kumanlioglu K and Akyildiz M. Prognostic factors of survival and recurrence pattern in differentiated thyroid cancer: a retrospective study from Western Turkey. Endocr Regul 2014; 48: 173-181.
[10] Lee CY, Kim SJ, Ko KR, Chung KW and Lee JH. Predictive factors for extrathyroidal extension of papillary thyroid carcinoma based on preoperative sonography. J Ultrasound Med 2014; 33: 231-238.
[11] Kim SS, Lee BJ, Lee JC, Kim SJ, Lee SH, Jeon YK, Kim BH, Kim YK and Kim IJ. Preoperative ultrasonographic tumor characteristics as a predictive factor of tumor stage in papillary thyroid carcinoma. Head Neck 2011; 33: 1719-1726.
[12] Wang QC, Cheng W, Wen X, Li JB, Jing H and Nie CL. Shorter distance between the nodule and capsule has greater risk of cervical lymph node metastasis in papillary thyroid carcinoma. Asian Pac J Cancer Prev 2014; 15: 855-860.
[13] Correas JM, Claudon M, Tranquart F and Helenon AO. The kidney: imaging with microbubble contrast agents. Ultrasound Q 2006; 22: 53-66.
[14] Waller KR, O'Brien RT and Zagzebski JA. Quantitative contrast ultrasound analysis of renal perfusion in normal dogs. Vet Radiol Ultrasound 2007; 48: 373-377.
[15] Jain RK. Normalizing tumor vasculature with anti-angiogenic therapy: a new paradigm for combination therapy. Nat Med 2001; 7: 987-989.
[16] Passe TJ, Bluemke DA and Siegelman SS. Tumor angiogenesis: tutorial on implications for imaging. Radiology 1997; 203: 593-600.
[17] Averkiou M, Powers J, Skyba D, Bruce M and Jensen S. Ultrasound contrast imaging research. Ultrasound Q 2003; 19: 27-37.
[18] Bartolotta TV, Midiri M, Galia M, Runza G, Attard M, Savoia G, Lagalla R and Cardinale AE. Qualitative and quantitative evaluation of solitary thyroid nodules with contrast-enhanced ultrasound: initial results. Eur Radiol 2006; 16: 2234-2241.
[19] Gao Y, Zheng DY, Cui Z, Ma Y, Liu YZ and Zhang W. Predictive value of quantitative contrast-enhanced ultrasound in hepatocellular carcinoma recurrence after ablation. World J Gastroenterol 2015; 21: 10418-10426.
[20] Han ML, Chen CC, Kuo SH, Hsu WF, Liou JM, Wu MS and Wang HP. Predictors of in-hospital mortality after acute variceal bleeding in patients with hepatocellular carcinoma and concurrent main portal vein thrombosis. J Gastroenterol Hepatol 2014; 29: 344-351.
[21] Yang YL, Yang RJ, Liu X, Liu J, Chao LJ and Duan YY. Correlations between the time-intensity parameters of contrast-enhanced ultrasound and clinical prognosis of hepatocellular carcinoma. Clin Imaging 2013; 37: 308-312.
[22] Kong WT, Wang WP, Huang BJ, Ding H and Mao F. Value of wash-in and wash-out time in the diagnosis between hepatocellular carcinoma and other hepatic nodules with similar vascular pattern on contrast-enhanced ultrasound. J Gastroenterol Hepatol 2014; 29: 576-580.
[23] Liu J, Gao YH, Li DD, Gao YC, Hou LM and Xie T. Comparative study of contrast-enhanced ultrasound qualitative and quantitative analysis for identifying benign and malignant breast tumor lumps. Asian Pac J Cancer Prev 2014; 15: 8149-8153.